IN-SITU SENSING OF ELASTIC AND PLASTIC DEFORMATION BEHAVIOR IN EPOXY-BASED STRAIN SENSOR USING VERTICALLY ALIGNED CARBON NANOTUBE GROWN ON SIC

Weikang. Li, Jinbo Bai*

Laboratoire de Mécanique des Sols, Structures et Matériaux, Ecole Centrale Paris, CNRS, UMR8579,PRES UniverSud, Grande Voie des Vignes, 92290 Châtenay-Malabry,France
jinbo.bai@ecp.fr

Keywords: *In-situ* sensing; carbon nanotube; deformation

Abstract
The multi-scale hybrid structure with vertically aligned carbon nanotubes (CNTs) grown on SiC microplate was achieved using chemical vapor deposition method. A high degree of carbon nanotube dispersion was obtained in the CNT-SiC/epoxy composites with an electrical percolation threshold (0.120 vol.%). The CNT-SiC hybrids could successfully serve as potential strain sensors. In-situ electrical resistance of CNT-SiC/epoxy composites linearly increased with strain in elastic region and then started to decrease when it entered into plastic region. This distinctive behavior of the resistance change could be applied to obviously identify elastic and plastic deformation in the composites, which was failed in the randomly orientated CNTs filled composites only with monotonic increase of electrical resistance until ultimate fracture.

1 Introduction

With their superior mechanical and electrical properties, carbon nanotubes (CNTs) can serve as not only the structural reinforcement but also the excellent *in situ* sensor in structural composites [1-3]. One of the challenges in using carbon nanotube network for damage sensing is how to disperse carbon nanotubes in polymer matrix. Recently, some researches about the hybrid structures consisting of CNTs and micrometer particles have shown that the CNT distribution and organization can be well controlled by optimizing the nano/micrometer hybrid structures in the matrix [4,5]. In our previous work, nano-micro hybrids has been obtained by *in situ* grafting of CNTs with different architectures on spherical alumina or SiC microparticles using chemical vapor deposition (CVD), where these particles provide efficient structures to improve the dispersion of CNTs within the polymer matrix [6-8]. However, to date, the use of hybrids with well-controlled CNTs as damage sensor has not been addressed on yet. Most of the available investigations on the damage sensor are limited to randomly orientated CNTs. When subjected to tensile stress, electrical resistance of the composites usually increased monotonically until the catastrophic failure [9-12]. There is still no obvious information to identify the elastic and plastic deformation of the composites by using these prevalent CNTs as damage sensor. Obviously, it is desirable that the multiform hybrid architectures constituted of well-organized CNTs mentioned above could solve this urgent issue. In our work, CNT-SiC nano/micro hybrids with vertically aligned CNTs grown on SiC microplate was proposed as damage sensor. Such hybrid structure is obtained by the self-

organization of carbon nanotubes on SiC microplate via chemical vapor deposition (CVD) synthesis. The epoxy composites based on CNT-SiC hybrids were fabricated and conducted a coupled electro-mechanical measurement. Very low fraction of vertically aligned CNTs (0.120 vol.%) could form electrically percolating networks. The *in situ* resistance change of the CNT-SiC/epoxy composites in the elastic and plastic regions was focused on. The percolating networks of CNT-SiC hybrids could be applied to successfully identify elastic and plastic region in the composites, which has usually been failed by using the traditional randomly oriented CNTs.

2 Materials and experimental process

Vertically aligned carbon nanotubes (CNTs) were synthesized on SiC microplates by a chemical vapor deposition (CVD) method. SiC microplates (Arion Technologie) with size of about 1μm were employed as substrate for CNT growth. Acetylene (C_2H_2) was selected as carbon source and ferrocene Fe $(C_5H_5)_2$ as catalyst precursor. A low-magnification SEM image Fig. 1a gives the whole morphology of each CNT-SiC hybrid. CNTs vertically aligned on the surface of SiC microplates, which can be clearly seen in the enlarged inset image. The thickness of the SiC microplate is about 1μm and the length of CNTs is about 10-15μm. Thermogravimetric analysis (TGA) shows that the mass fraction of CNTs in CNT-SiC hybrids is about 30% (see Fig. 1b).

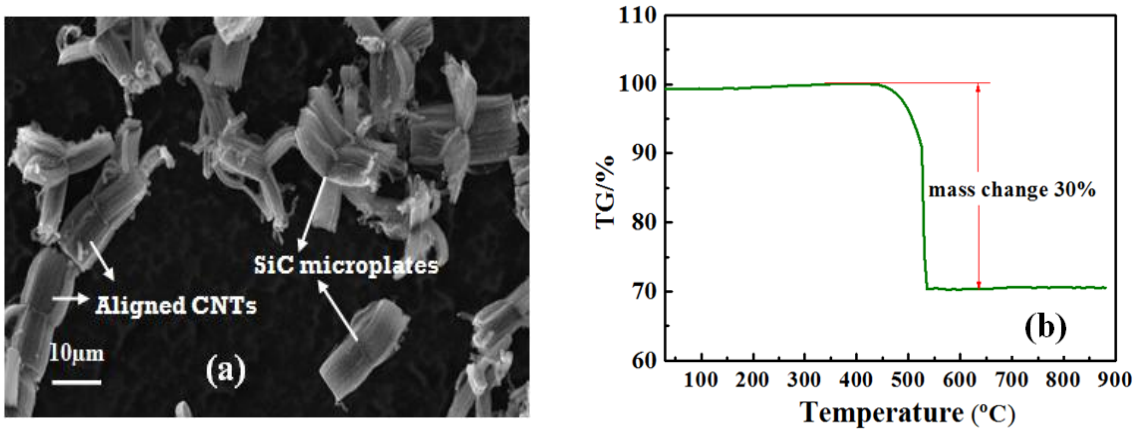

Figure 1. (a) SEM image and **(b)** Thermogravimetric analysis (TGA) of the CNT-SiC hybrids.

The CNT-SiC hybrids were dispersed in epoxy resin using a three-roll mill following a well-established protocol, where the gaps between adjacent rollers were set as 25μm. The mixture was degassed for 20min and curing agent (1084, Resoltech Ltd, at a ratio of 1/3 to epoxy resin) was added to the dispersion. Subsequently, the resulting epoxy matrix composites were cured at 60°C under 10Mpa for 3 h. Dumbbell-shape samples with 1.0 mm in thickness, 50.0 mm in length, and 12.0 and 4.0 mm in maximal and minimal widths were obtained and edge-polished for tensile testing.

The fracture surfaces were observed using a field emission SEM (Germany ZEISS, LEO 1530 Gemini). Prior to measurement, silver paste electrodes were applied to both sides of the samples in order to reduce the contact resistance. Quasi-static and incremental cyclic tensile tests were carried out in a micro-tensile machine (Instron 5544) at a fixed displacement rate of 0.2mm/min. For cyclic loading, the specimens were loaded and un-loaded at the same rate with progressively increasing peak values of cyclic load. A Keithley 2400voltage-current meter was used to measure the in-plane volume electrical resistance of the specimens by sourcing a constant voltage of 20 V and measuring the current using a two-probe method. The electrical contact resistance is very small relative to the overall specimen resistance due to the nature of these specimens. All the resistance, strain, and load data were recorded using data acquisition software written by Lab View.

3 Results

3.1 Microstructure of the composites

Fig. 2 shows SEM images of the fracture surface of the epoxy composites based on CNT-SiC hybrids. It can be seen that the original architecture of CNT-SiC hybrid is retained after being mixed with epoxy (Fig. 2a) and the CNTs grown on SiC microplate shows good dispersion in the epoxy matrix which offered wide conducting space or more conducting path (Fig. 2b). This CNT distribution may mainly influence the conduction mechanism of the two composite.

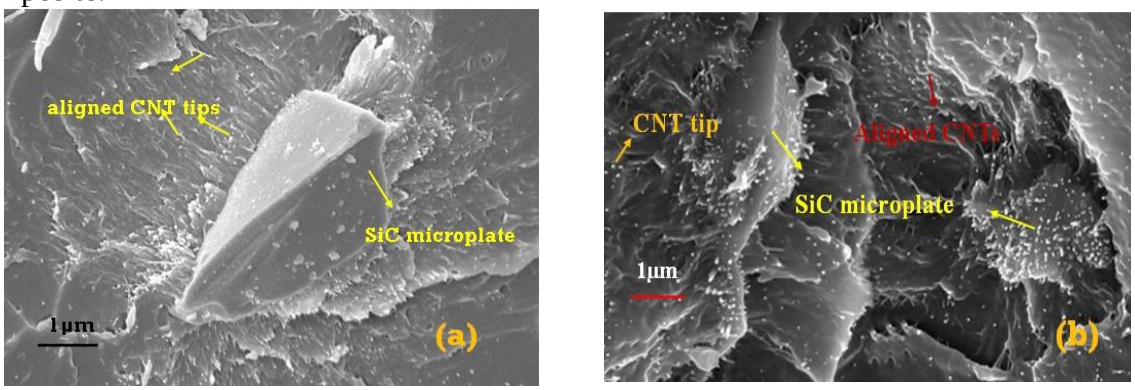

Figure 2. SEM images of the CNT-SiC/epoxy composites.

3.2 dc conductivity of the composites

To reach the percolation threshold, the epoxy composites with different volume fractions of CNT-SiC hybrids are fabricated. Fig. 3 shows the dc conductivity versus the volume fraction of conductive fillers in the CNT-SiC/epoxy composites. A moderate increase in conductivity is observed when the volume fraction of conductive filler is below the percolation threshold, while it becomes significant after the volume fraction is above the percolation threshold. The variation of conductivity shows a good agreement with the typical power law [2]:

$$\sigma \propto (f - f_c)^t \qquad as \qquad f > f_c \tag{1}$$

Where, σ, f, f_c and t are the conductivity of the composite, volume fraction of the fillers, percolation threshold and critical exponent in the conducting region which depends on the dimensionality of the conductive network. In our research about the CNT-SiC/epoxy system, f is the volume fraction of the CNT instead of the hybrids. The best fits of the experimental

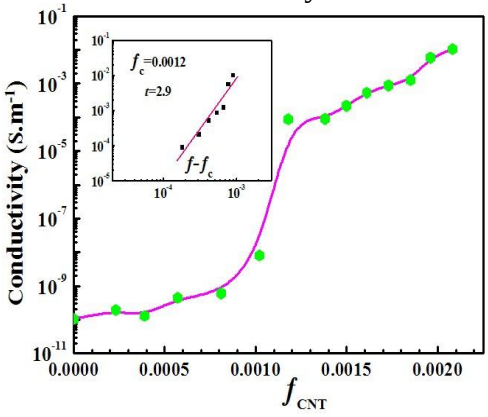

Figure 3. DC conductivities of the CNT-SiC/epoxy composites as a function of the CNT volume content. The insets show the best fit of the dc electrical conductivities of the composites to Eq. (1).

conductivity data to the log-log plots of the power laws give f_c =0.0012 and t=2.9 (see the insets in Fig. 3). The critical exponent of the two system exhibits higher values than the universal ones (1.6~2 for a three-dimensional network and ≈1.43 for two-dimensional

network), respectively [13]. According to the value of critical exponent, we can conclude that the high degree of carbon nanotube distribution can efficiently increase its utilization ratio in forming conducting network at lower loading.

3.3 Mechanical behavior and strain-dependent resistance characterization

Fig. 4 demonstrates the characteristic stress ~ strain (σ ~ ε) response curves (solid lines) and the corresponding strain-dependent resistance change (dotted lines) of the epoxy-based composites with various contents of CNT-SiC hybrids under quasi-static loading. In view of potential applications on strain sensing materials, strain sensitivity is defined as gauge factor (k). It is the slope of the linear region and expressed as [10]

$$\frac{\Delta R_1}{R_o} = k\varepsilon \tag{2}$$

The sensitivities of damage in the composites decrease with the increase of the CNT-SiC content.

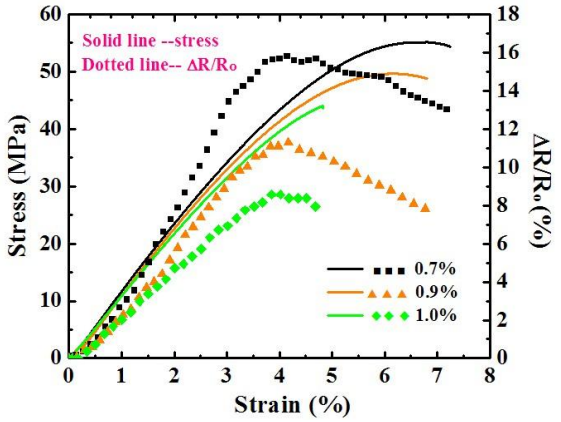

Figure 4. Stress-strain and resistance-change response curves of the CNT-SiC/epoxy composites with different contents of CNT-SiC hybrids under quasi-static loading.

A detailed research of the characteristic stress ~ strain response curve and the corresponding resistance-change of the epoxy composite with 0.7 wt% CNT-SiC hybrids is shown in Fig. 5. The resistance monotonically increases then begins to decrease when the strain passes a critical value ε_r, which obviously divides the dotted line into Region I and II.

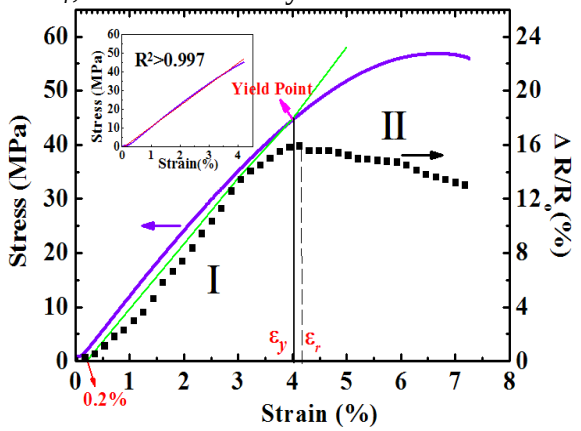

Figure 5. Stress-strain and resistance-change response curves of the CNT-SiC/epoxy composites with 0.7 wt% CNT-SiC hybrids under quasi-static loading.

The stress-strain curve (0~ε_r) displays a typical linear-elastic behavior (see the inset), which is reconciled with the well-known Hooke's Law. Traditionally, the elastic and plastic region could be identified via offset yield point. A 0.2% offset strain has been taken to define the offset yield point (Y). In order to further verify the yield point, the specimen is also subjected to an incremental tensile cyclic test as shown in Fig. 6. At the first third cycles, though the

damage is initiated and there is crack re-open in each subsequent cycle, elastic deformation followed by new crack formation could be identified in the resistance-change curve. During the fourth cycle, there is a larger resistance change upon re-loading and also a permanent resistance appears change in the unloaded state due to the plastic deformation of the composites (see Fig. 6b). That is, once the yield point where $\sigma_y \approx 46$ MPa is passed, the plastic deformation happened. Meanwhile, the corresponding ε_y is very close to ε_r. As a result, this *in situ* sensing behavior of our CNT-SiC hybrids in the composites could offer valuable information for identifying the elastic and plastic region.

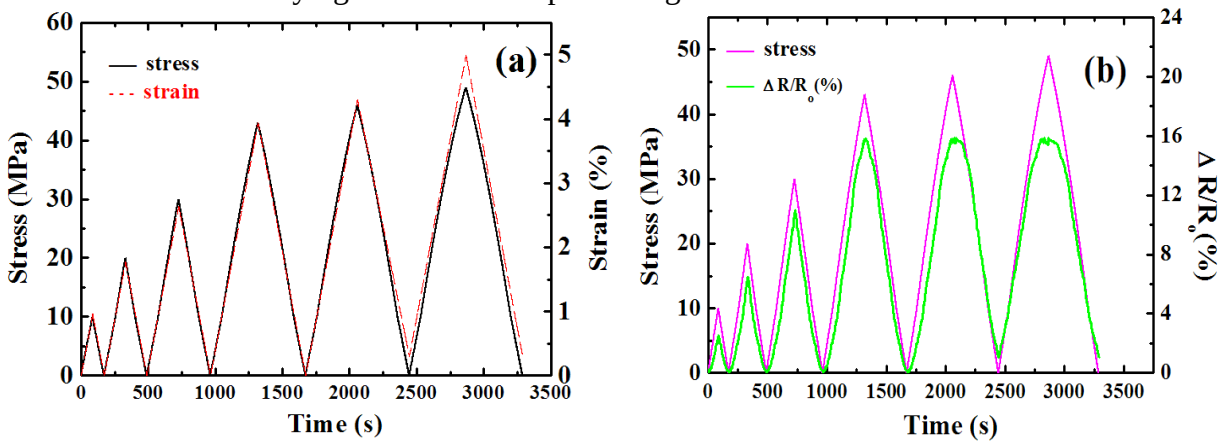

Figure 6. Stress-strain and resistance-change response curves of the CNT-SiC/epoxy composites with 0.7 wt% CNT-SiC hybrids under incremental cyclic loading.

Before tensile loading, the vertically aligned CNTs well dispersed in the matrix and the conductive networks are formed (Fig. 7a). In the elastic region, the elastic deformation makes the number of contact points between CNTs on different SiC microplates decrease (Fig. 7b). As a result, the *in situ* electrical resistance increases in this region. When the plastic deformation occurs, there is reformation of the conductive networks after their break-ups, which can be explained by the electrical tunneling resulted from the closing of the micro-cracks because of Poisson's contraction [14]. There is a good dispersion of the vertically aligned CNTs and two neighboring CNTs grown on SiC are not overlapping yet still situated closely enough to allow electrical tunneling, which is different from the case of randomly orientated CNTs. Besides, Poisson's ratio effect and the intense movement of the polymer chain may result in the rotation of some CNT bundles grown on SiC along the stress direction (Fig. 7e). This rotation of CNT bundle is different from that of randomly orientated CNTs because only free ends of them could be rotated and the other ends are attached to SiC microplate. Besides, the possible reorientation of the SiC microplate could not be seen from the optical image because the SiC microplate is much smaller compared to the CNTs. Therefore, it is possible for this kind of nano/micro hybrid to reform the conductive networks in the plastic region (Fig. 7c). This may explain the decrease of electrical resistance when it entered into the plastic region.

4 Conclusion

Electrically conductive epoxy composites with CNT-SiC nano/micro hybrids and randomly orientated carbon nanotubes were comparably studied concerning their potential applications for strain sensors. The strain-dependent electrical resistance of the CNT-SiC/epoxy composites could be applied to identify the elastic and plastic region. This in situ sensing behavior was failed in the randomly orientated CNTs/epoxy composites only with monotone increase of electrical resistance until ultimate fracture. Therefore, it becomes possible to limit the composites within the elastic region using their in situ resistance change which hold very promise for the safe use of composites as structural components.

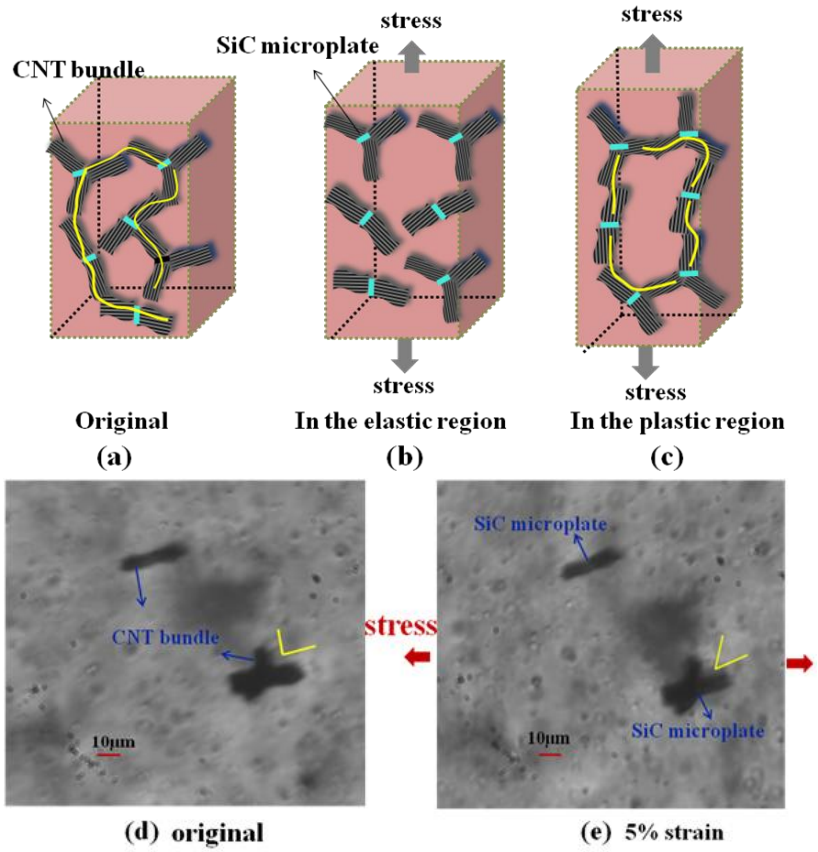

Figure 7. (a)~(c) Schematics of evolution of the conductive networks; **(d), (e)** Optical images of CNT-SiC hybrids during tensile loading. The dotted line represents the conductive networks.

References

[1] Li C, Thostenson ET, Chou TW. Sensors and actuators based on carbon nanotubes and their composites: A review. *Compos Sci Technol*, **68**, 1227-1249 (2008).

[2] Dang ZM, Yuan JK, Zha JW, Zhou T, Li ST, Hu GH. Fundamentals, process and applications of high-permittivity polymer-matrix composites. *Prog Mater Sci*, **57**, 660-723 (2012).

[3] Oliva-Avilés AI, Avilés F, Sosa V. Electrical and piezoresistive properties of multi-walled carbon nanotube/polymer composite films aligned by an electric field. *Carbon*, **49**, 2989-2997 (2011).

[4] Georgakilas V, Gournis D, Tzitzios V, Pasquato L, Guldi DM, Prato M. Decorating carbon nanotubes with metal or semiconductor nanoparticles. *J Mater Chem*, **17**, 2679-2694 (2007).

[5] Thostenson ET, Li WZ, Wang DZ, Ren ZF, Chou TW. Carbon nanotube/carbon fiber hybrid multiscale composites. *J Appl Phys*, **91**, 6034-6037 (2002).

[6] Bozlar M, He D, Bai J, Chalopin Y, Mingo N, Volz S. Carbon nanotube microarchitectures for enhanced thermal conduction at ultralow mass fraction in polymer composites. *Adv Mater*, **22**, 1654-1658 (2010).

[7] Ci L, Bai J. Novel Micro/Nanoscale Hybrid Reinforcement: Multiwalled Carbon Nanotubes on SiC Particles. *Adv Mater*, **16**, 2021-2024 (2004).

[8] He D, Bozlar M, Genestoux M, Bai J. Diameter- and length-dependent self-organizations of multi-walled carbon nanotubes on spherical alumina microparticles. *Carbon*, **48**, 1159-1170 (2010).

[9] Thostenson ET, Chou TW. Real-time in situ sensing of damage evolution in advanced fiber composites using carbon nanotube networks. *Nanotechnology*, **19**, 215713 (2008).

[10] Park M, Kim H, Youngblood JP. Strain-dependent electric resistance of multi- walled carbon nanotubes//polymer composite films. *Nanotechnology*, **19**, 055705 (2008).
[11] Zhang R, Baxendale M, Peijs T. Universal resistivity-strain dependence of carbon nanotube/polymer composites. *Phys Rev B*, **76**, 195433 (2007).
[12] Hu N, Karube Y, Arai M, Watanabe T, Yan C, Li Y, et al. Investigation on sensitivity of a polymer/carbon nanotube composite strain sensor. *Carbon*, **48**, 680-687 (2010).
[13] Du J, Zhao L, Zeng Y, Zhang L, Li F, Liu P, et al. Comparison of electrical properties between multi-walled carbon nanotube and graphene nanosheet/high density polyethylene composites with a segregated network structure. *Carbon*, **49**, 1094-1100 (2011).
[14] Kim KJ, Yu WR, Lee JS, Gao L, Thostenson ET, Chou TW, et al. Damage characterization of 3D braided composites using carbon nanotube-based in situ sensing. *Compos Part A-Appl S*, **41**, 1531-1537 (2010).